Chaotic instabilities in smectic-C liquid crystals

I. W. Stewart,[1,*] T. Carlsson,[2] and F. M. Leslie[3]
[1]Department of Theoretical Mechanics, University of Nottingham, University Park, Nottingham NG7 2RD, England
[2]Physics Department, Chalmers University of Technology, S-412 96 Göteborg, Sweden
[3]Department of Mathematics, University of Strathclyde, Livingstone Tower, 26 Richmond Street, Glasgow G1 1XH, Scotland
(Received 7 July 1993)

An investigation is made of chaos in planar samples of nonchiral smectic-C liquid crystals. When a static electric field is applied at an oblique angle to the layers an explicit solitonlike solution is derived from the smectic continuum equations: this solution describes a moving domain wall. When a suitable oscillating electric field is superimposed on the static field this domain wall can be unstable and chaotic instabilities are shown to arise in the movement of the c director. Criteria for the onset of chaos are provided via a Melnikov analysis where, for example, for any given smectic tilt angle it can be decided which magnitudes and frequencies of the oscillating field lead to chaos.

PACS number(s): 61.30.Cz, 47.52.+j

I. INTRODUCTION

Liquid crystals consist of elongated molecules for which the long molecular axes locally adopt one common direction in space, generally described by a unit vector **n** called the director. Smectic-C liquid crystals are layered structures for which the director is tilted by an angle θ with respect to the layer normal. In this work it is assumed that the layers are of constant thickness. The unit layer normal is denoted by **a** and, as introduced by de Gennes [1], a unit vector **c** (the *c* director), which is perpendicular to **a**, is used to describe the direction of the average molecular tilt of the alignment with respect to the layer normal. The *c* director is parallel to the projection of the usual director **n** onto the smectic planes (see Fig. 1).

Smectic-C liquid crystals can form planar layers in the bulk where the two directors **a** and **c** are constant in space. Applying an external electric field to a homogeneous sample can, for proper combinations of the boundary conditions imposed on the *c* director at the surrounding glass plates and the direction of the applied field, result in a Fréedericksz transition where the *c* director may rotate around the layer normal while the layers remain intact; static and moving domain walls are also possible and do not disturb the layer structure. Layer distortions may also occur. The combinations of the possible deformations involving perturbations of the *a* and *c* directors are associated with an elastic energy having nine elastic constants (see Refs. [1–4]). From this continuum theory the elastic constant B_3 and the rotational viscosity λ_5 will appear in the equations discussed below in Sec. II; much of the analysis is motivated by the known solutions for static and moving domain walls presented in Stewart and Raj [5] and Schiller, Pelzl, and Demus [6].

The derivation of the dynamic equation we will use is given in the Appendix, together with a brief outline of the theory contained in [4]. Simpler heuristic derivations are possible, but the techniques employed in the Appendix (involving Lagrange multipliers) are of great mathematical convenience when considering more complicated layered structures of smectic-C liquid crystals such as the focal conics (see de Gennes [1]). The use of these multipliers has been successfully demonstrated by Nakagawa [7] and Stewart, Nakagawa, and Leslie [8] and it is in anticipation of their usefulness for the future that more detailed manipulations have been included in the Appendix.

The onset of chaotic motions of the *n* director in nematic liquid crystals has been discussed by Abdullaev, Abdumalikov, and Tsoi [9]. The aim of this article is to show that chaotic solutions can occur when an electric field, composed of a static field that is augmented by a weak low-frequency alternating field, is applied at a small tilted angle to the planes of a planar aligned sample of

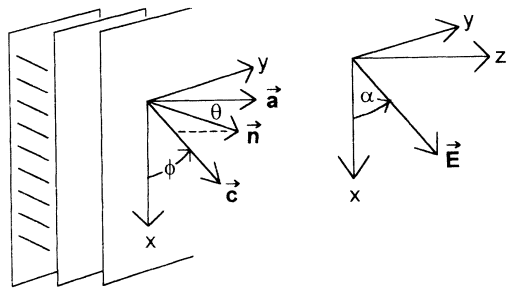

FIG. 1. The average molecular alignment, i.e., the director, is prescribed by a unit vector **n** making an angle θ with the layer normal **a**. The *c* director is the unit vector parallel to the projection of the *n* director onto the smectic planes and is denoted by **c**. The *z* axis is taken to coincide with the orientation of the layer normal **a** and the *x* and *y* axes lie within the smectic planes. The electric field **E** makes an angle α with the smectic planes as shown in the figure.

*Author to whom correspondence should be addressed.

nonchiral smectic-C liquid crystal. Instabilities in the form of chaos arise from the oscillatory forcing term due to the alternating field; when the alternating field is absent and only the static field is present an explicit solitonlike solution is available.

II. DESCRIPTION OF THE PROBLEM

A. Geometrical arrangement, energies, and the dynamic equation

We consider a nonchiral smectic-C liquid crystal in the bulk where the planar smectic layers of constant thickness are aligned as shown in Fig. 1. The layer normal $\mathbf{a}$ is taken to be parallel to the z axis. The average direction of the molecules is described by the unit vector $\mathbf{n}$, the director, and θ is the usual temperature-dependent smectic tilt angle ($\cos\theta=\mathbf{n}\cdot\mathbf{a}$), for our purposes assumed constant. The xy plane is taken to be parallel to the smectic planes and the c director, being the unit projection of the director into the smectic planes, is described by the phase angle ϕ, as indicated in Fig. 1.

Using the above notation, the two directors $\mathbf{a}$ and $\mathbf{c}$ are subject to the constraints

$$\mathbf{a}\cdot\mathbf{a}=\mathbf{c}\cdot\mathbf{c}=1,\quad \mathbf{a}\cdot\mathbf{c}=0\ . \tag{2.1}$$

Further, as dislocations are not considered, we require (Oseen [10])

$$\nabla\times\mathbf{a}=\mathbf{0}\ . \tag{2.2}$$

The bulk energy integrand involving the gradients of $\mathbf{a}$ and $\mathbf{c}$ can be written in the equivalent forms

$$w=w(\mathbf{a},\mathbf{c},\nabla\mathbf{a},\nabla\mathbf{c})=w(\mathbf{b},\mathbf{c},\nabla\mathbf{b},\nabla\mathbf{c})\ , \tag{2.3}$$

where $\mathbf{b}=\mathbf{a}\times\mathbf{c}$ and the symmetry of the nonchiral smectics results in a nine-term quadratic bulk energy as given in the Appendix [Eq. (A1)].

An electric field $\mathbf{E}$ is introduced, making a small angle $\alpha>0$ with the smectic planes

$$\mathbf{E}=E_0(\cos\alpha,0,\sin\alpha)\ , \tag{2.4}$$

where $E_0=|\mathbf{E}|$ is the strength of the electric field. We make the following ansatz for $\mathbf{a}$, $\mathbf{c}$, and $\mathbf{n}$:

$$\mathbf{a}=(0,0,1)\ , \tag{2.5a}$$

$$\mathbf{c}=(\cos\phi(z,t),\sin\phi(z,t),0)\ , \tag{2.5b}$$

$$\mathbf{n}=\mathbf{a}\cos\theta+\mathbf{c}\sin\theta\ , \tag{2.5c}$$

motivated by looking at the possible orientation of $\mathbf{c}$ as a function of z and time t when $\alpha\neq0$. For the above choice of $\mathbf{a}$ and $\mathbf{c}$ with this supposed spatial and time dependence [satisfying constraints (2.1) and (2.2)] the resulting bulk energy integrand, by Eq. (A1), becomes

$$w=\tfrac{1}{2}B_3[\tfrac{1}{2}(\mathbf{b}\cdot\nabla\times\mathbf{b}+\mathbf{c}\cdot\nabla\times\mathbf{c})]^2=\tfrac{1}{2}B_3\left[\frac{\partial\phi}{\partial z}\right]^2\ , \tag{2.6}$$

where B_3 is the positive elastic constant related to the rotation of the c director as we move from layer to layer, $\mathbf{c}$ having the same orientation within each individual layer (see Carlsson, Stewart, and Leslie [2] for a description and discussion of this and other related deformations).

The electric free-energy density that occurs when an electric field is applied across a liquid crystal may be written as [1]

$$w^e=-\tfrac{1}{2}\varepsilon_a\varepsilon_0(\mathbf{n}\cdot\mathbf{E})^2\ , \tag{2.7}$$

where ε_0 is the permittivity of free space and ε_a is the dielectric anisotropy of the liquid crystal, assumed in this work to be positive. Imposing the above geometry, Eqs. (2.4) and (2.5) show that

$$w^e=-\tfrac{1}{2}\varepsilon_a\varepsilon_0E_0^2[\sin\alpha\cos\theta+\cos\alpha\sin\theta\cos\phi(z,t)]^2 \tag{2.8}$$

and we therefore set

$$W=w+w^e\ . \tag{2.9}$$

Before deriving the dynamic equation of the system we study the physical implication of the dielectric potential (2.8) in a qualitative way. Provided that $\varepsilon_a>0$ and $\alpha<\theta$, this potential exhibits two local minima for $\phi=0,\pi$ as depicted in Fig. 2. If $\alpha=0$ (the electric field being parallel to the smectic planes) the two minima are of equal depth and the system is bistable. If the electric field makes an angle $\alpha>0$ with the smectic planes, the minimum $\phi=\pi$ is metastable [$w^e(\phi=\pi)>w^e(\phi=0)$]. Now consider a system with two domains separated by a π wall as depicted in Fig. 3. If the electric field is applied parallel to the smectic planes ($\alpha=0$) both the domains $\phi=0$ and $\phi=\pi$ have the same dielectric energy and the wall is fixed. If, instead, the field makes an angle with the smectic planes the domain $\phi=\pi$ has a large dielectric energy than the

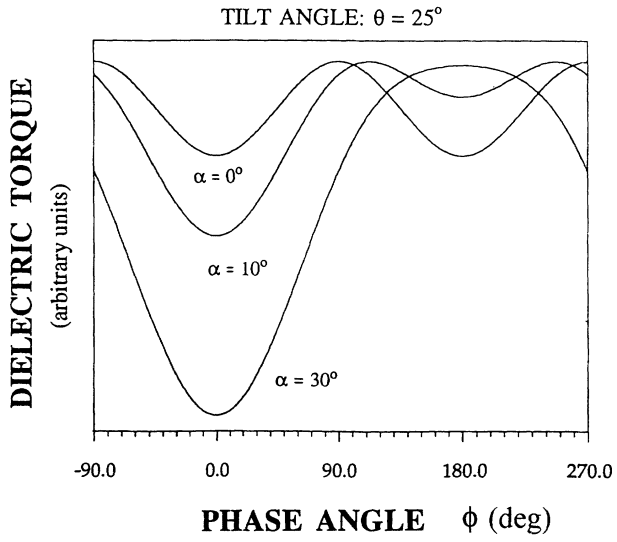

FIG. 2. Dielectric potential w^e [Eq. (2.8)] as a function of the phase angle ϕ for three different values of the angle α between the electric field and the smectic planes. When $\alpha=0$ the potential exhibits two minima of equal depth at $\phi=0$ and $\phi=\pi$ and the system is bistable. If $0<\alpha<\theta$ then the minimum at $\phi=\pi$ has the larger dielectric energy and the system becomes metastable. Finally, when $\alpha>\theta$, the minimum at $\phi=\pi$ disappears and instead becomes a maximum.

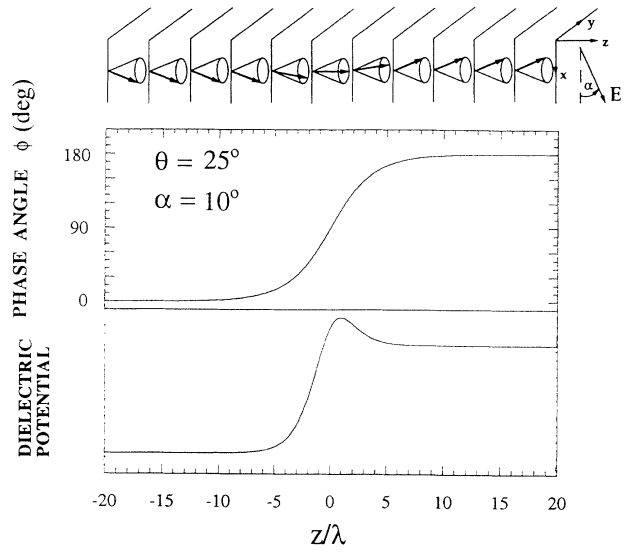

FIG. 3. Snapshot of the propagating domain wall [Eq. (2.14)] at $t=0$. The upper part of the figure shows how the director rotates around the smectic cone in the region between the stable ($\phi=0$) and the metastable ($\phi=\pi$) domains. The middle part of the figure depicts $\phi(z,0)$ and it is seen how the wall, having a thickness of the order $\lambda/(\sin\theta\cos\alpha)$, is located around $z=ut$. In the lower part of the figure the dielectric potential [Eq. (2.8)] corresponding to $\phi(z,0)$ is depicted. When time increases the wall propagates to the right, driven by the dielectric and elastic torques which are due to the asymmetry of the c-director profile around $z=ut$.

domain $\phi=0$. In this case the wall will propagate through the system, driven by the electric and dielectric torques, in a direction which makes the $\phi=0$ domain expand at the cost of the $\phi=\pi$ domain.

Minimizing the energy (2.9) using the Euler-Lagrange equations as discussed in the Appendix [leading to Eq. (A15)] results in the dynamic equation

$$B_3\frac{\partial^2\phi}{\partial z^2}-2\lambda_5\frac{\partial\phi}{\partial t}-\varepsilon_a\varepsilon_0E_0^2(\sin\alpha\cos\theta+\cos\alpha\sin\theta\cos\phi)\times\cos\alpha\sin\theta\sin\phi=0\ . \quad (2.10)$$

Here λ_5 is the positive rotational viscosity related to the movement of the director $\mathbf{n}$ around a cone whose semivertical angle is the smectic tilt angle θ. The solution of (2.10) for $\phi(z,t)$ will lead to complete solutions for the Euler-Lagrange equations as discussed in the Appendix, as required. The solution ϕ will further enable the Lagrange multipliers arising from the constraints (2.1) and (2.2) to be calculated explicitly if necessary via the relevant equations derived in the Appendix (for example, the onset of layer deformations may require a more detailed analysis of the behavior of the constraints).

Equation (2.10) can be interpreted as a balance-of-torque equation where the B_3 term represents the elastic torque which is due to the rotation of the c director when going from one layer to another. The λ_5 term is the rotational torque, being proportional to the angular velocity $d\phi/dt$ of the c director, while the last term in the equation represents the dielectric torque. As it is written, Eq. (2.10) represents the z component of the three-dimensional balance-of-torque equation. This equation is the governing equation for $\phi(z,t)$ derived by the mathematical theory presented in the Appendix. We would like to point out that some debate today exists in the literature regarding the choice of the z component of the torque equation as the governing equation of the system. A more physical approach, such as that by Carlsson, Leslie, and Clark [11], suggests that the proper component of the torque equation governing the rotation of the c director in the system we are studying may be the θ component, where instead of a Cartesian coordinate system a spherical polar coordinate system is employed to describe the director. One possible explanation of the discrepancy between the two approaches is discussed in Ref. [11]. Since the two approaches give qualitatively similar equations of motion for the system, in this paper we will be content with analyzing the rotation of the c director as it is given by Eq. (2.10), leaving the choice of the proper component of the torque equation aside for the moment.

Before analyzing Eq. (2.10) we note that it can be rewritten as

$$\lambda^2\frac{\partial^2\phi}{\partial z^2}-t_0\frac{\partial\phi}{\partial t}=(\sin\alpha\cos\theta+\cos\alpha\sin\theta\cos\phi)\cos\alpha\sin\theta\sin\phi\ . \quad (2.11)$$

Here we have introduced λ and t_0, which represent a typical length scale and time scale in the problem, respectively, and are given by

$$\lambda=\frac{1}{E_0}[B_3/(\varepsilon_a\varepsilon_0)]^{1/2}\ , \quad (2.12)$$

$$t_0=2\lambda_5/(\varepsilon_a\varepsilon_0E_0^2)\ . \quad (2.13)$$

Following the solution of Schiller, Pelzl, and Demus [6] (with a suitably redefined α), Eq. (2.11) is known to have solitonlike solutions for $\alpha\neq0$ which describe a moving domain wall, namely,

$$\phi(z,t)=2\tan^{-1}\left[\exp\left[\frac{\pm(z-ut)}{\lambda}\sin\theta\cos\alpha\right]\right] \quad (2.14)$$

for which the velocity of the wall is

$$u=\pm\frac{\lambda}{t_0}\sin\alpha\cos\theta\ . \quad (2.15)$$

The wall corresponding to the plus sign in Eq. (2.14) is the one described qualitatively in Fig. 3, while the negative sign corresponds to a wall moving to the left in a system for which the $\phi=0$ and $\phi=\pi$ domains have changed places. The solution (2.14) is available whenever $\mathbf{E}$ is a static field: for the remainder of this paper an examination will be made of possible solutions to (2.11) when a slowly oscillating ac field is gradually combined with a fixed static field.

B. Approximations and equations involving a superimposed ac field

We assume that the tilted field angle is small, that is,

$$0<\alpha\ll 1 , \tag{2.16}$$

and seek solutions to Eq. (2.10) when the static field considered above is gradually augmented with an appropriate ac field possessing a slowly varying frequency. This is achieved by replacing E_0 in (2.10) by

$$E_0\rightarrow E_0[1+(\varepsilon/2)\cos(\omega\varepsilon t)] , \tag{2.17}$$

where $\omega\varepsilon$ is the frequency of the superimposed field and ε is suitably small. To make the problem more tractable we will suppose that

$$\varepsilon=\xi\alpha \tag{2.18}$$

for some positive constant ξ. The assumptions (2.16)–(2.18) lead to the substitution

$$E_0^2\rightarrow E_0^2[1+\xi\alpha\cos(\omega\xi\alpha t)] \tag{2.19}$$

in Eq. (2.11), which is then straightforwardly rewritten as

$$\lambda^2\frac{\partial^2\phi}{\partial z^2}-t_0\frac{\partial\phi}{\partial t}=\tfrac{1}{2}\{\alpha\sin(2\theta)\sin\phi +[1+\xi\alpha\cos(\omega\xi\alpha t)] \times\sin^2\theta\sin(2\phi)\} . \tag{2.20}$$

Motivated by the solution under a static field given in Eq. (2.14), solutions to (2.20) of the type

$$\phi(z,t)=\phi(\tau) , \qquad \tau=\frac{z}{\lambda}\sin\theta-\frac{t}{t_0}\alpha\sin^2\theta+d \tag{2.21}$$

will be sought, where the constants λ and t_0 are given by Eqs. (2.12) and (2.13) and d is an arbitrary constant. Equation (2.20) may be regarded as a special approximation to a perturbation of the static-field solution in (2.11). It follows that

$$\frac{\partial^2}{\partial z^2}=\frac{\sin^2\theta}{\lambda^2}\frac{d^2}{d\tau^2} \quad\text{and}\quad \frac{\partial}{\partial t}=-\frac{\sin^2\theta}{t_0}\alpha\frac{d}{d\tau} . \tag{2.22}$$

The time behavior of solutions will be examined for a given suitably small region around an arbitrary point z_0, say, noting that whenever $\alpha>0$, $\tau\rightarrow\pm\infty$ corresponds to $t\rightarrow\mp\infty$. Setting $d=-(\sin\theta/\lambda)z_0$ in Eq. (2.21) shows that

$$\alpha\cos(\omega\xi\alpha t)=\alpha\cos(\bar{\omega}\tau) , \tag{2.23}$$

where

$$\bar{\omega}=\frac{\omega\xi t_0}{\sin^2\theta} \tag{2.24}$$

whenever

$$|z-z_0|\le\frac{\alpha\lambda}{t_0\omega\xi}\sin\theta , \tag{2.25}$$

that is, whenever the solution is investigated sufficiently near the original point z_0. Equations (2.22)–(2.24) allow (2.20) to be written as

$$\frac{d^2\phi}{d\tau^2}+\alpha\frac{d\phi}{d\tau}=\alpha\cot\theta\sin\phi+\tfrac{1}{2}[1+\xi\alpha\cos(\bar{\omega}\tau)]\sin(2\phi) , \tag{2.26}$$

which may be formulated as the first-order system

$$\frac{d}{d\tau}\begin{bmatrix}\phi\\ v\end{bmatrix}=\begin{bmatrix} v\\ \frac{1}{2}\sin(2\phi)\end{bmatrix} +\alpha\begin{bmatrix}0\\ -v+\cot\theta\sin\phi+(\xi/2)\cos(\bar{\omega}\tau)\sin(2\phi)\end{bmatrix} =\begin{bmatrix}f_1(\phi,v)\\ f_2(\phi,v)\end{bmatrix}+\alpha\begin{bmatrix}g_1(\phi,v,\tau)\\ g_2(\phi,v,\tau)\end{bmatrix} =\mathbf{f}(\phi,v)+\alpha\mathbf{g}(\phi,v,\tau) , \tag{2.27}$$

where $v=d\phi/d\tau$ and, for ease of notation later, the functions $\mathbf{f}(\phi,v)$ and $\mathbf{g}(\phi,v,\tau)$ are introduced as indicated above.

The remainder of this paper demonstrates the possibility that solutions to Eq. (2.27) can exhibit chaotic dynamics in a small enough neighborhood of the originally chosen point z_0. Since this choice of z_0 is arbitrary, we can conclude that chaos may be present everywhere in the liquid-crystal sample where the ac field is applied.

III. CHAOTIC DYNAMICS BY MELNIKOV'S METHOD

Equation (2.27) will now be analyzed via Melnikov's method and the techniques employed, for example, by Guckenheimer and Holmes [12] and Marsden [13]; the objective is to prove that there exist chaotic solutions in the sense of Smale horseshoes whenever $\alpha>0$ is sufficiently small. This is achieved by evaluating, and examining the behavior of, the Melnikov function (defined below) whose calculation requires the solution of the unperturbed system ($\alpha=0$). A statement of the relevant theory will be made below, while for full details and examples of Smale horseshoes, chaotic dynamics, and proofs of the Melnikov method the reader is referred to the references cited above.

The unperturbed system for (2.27) is

$$\frac{d}{d\tau}\begin{bmatrix}\phi\\ v\end{bmatrix}=\begin{bmatrix} v\\ \frac{1}{2}\sin(2\phi)\end{bmatrix} , \tag{3.1}$$

which has Hamiltonian H given by

$$H(\phi,v)=\tfrac{1}{2}v^2+\tfrac{1}{4}\cos(2\phi) \tag{3.2}$$

since

$$\frac{\partial H}{\partial v}=v \quad\text{and}\quad -\frac{\partial H}{\partial\phi}=\tfrac{1}{2}\sin(2\phi) . \tag{3.3}$$

The equilibria for the unperturbed system are, with the assumption that $\varepsilon_a>0$, clearly at $\phi=0$, $\pi/2$, π, etc., and, as the phase portrait in the ϕv plane repeats itself every

π, only the phase portrait for ϕ between 0 and π is considered. The heteroclinic orbits (separatrices in the phase plane) occur when $H \equiv \frac{1}{4}$, that is, when

$$v_+ = \sin\phi \quad \text{and} \quad v_- = -\sin\phi \ , \tag{3.4}$$

where the plus and minus signs represent the upper and lower separatrices in the plane, respectively. This pair of heteroclinic orbits is easily derived to be

$$\mathbf{q}^0_+(\tau) = (\phi^0_+, v^0_+) = (2\tan^{-1}[\exp(\tau)], \operatorname{sech}\tau) \ , \tag{3.5}$$

$$\mathbf{q}^0_-(\tau) = (\phi^0_-, v^0_-) = (\pi - 2\tan^{-1}[\exp(\tau)], -\operatorname{sech}\tau) \ , \tag{3.6}$$

where $-\infty < \tau < \infty$; the interior and exterior of $\mathbf{q}^0_+ \cup \mathbf{q}^0_-$ are filled with periodic orbits ($\phi = \pi/2$ is a center).

The wedge product of $\mathbf{f}$ and $\mathbf{g}$ is defined by

$$\mathbf{f} \wedge \mathbf{g} = f_1 g_2 - f_2 g_1 \tag{3.7}$$

and for the upper heteroclinic orbit we define the Melnikov function to be

$$M_+(\tau_0) = \int_{-\infty}^{\infty} \mathbf{f}(\mathbf{q}^0_+(\tau)) \wedge \mathbf{g}(\mathbf{q}^0_+(\tau), \tau + \tau_0) d\tau \ . \tag{3.8}$$

$M_-(\tau_0)$ is similarly defined for the lower orbit. The Melnikov function is, in some sense, a measure of the distance between the perturbed and unperturbed solutions. M_+ is said to have a simple zero at τ_1 if

$$M_+(\tau_1) = 0 \quad \text{and} \quad \frac{dM_+}{d\tau_0}(\tau_1) \neq 0 \ . \tag{3.9}$$

For $\alpha = 0$ the system (3.1) possesses heteroclinic orbits to the hyperbolic saddle point at $\phi = 0$; these conditions are sufficient for us to apply Melnikov's method for the existence of chaos ([14], p. 71), which we now state in a form suitable for our purposes (see [12,13]):

Theorem. If $M_+(\tau_0)$ [or $M_-(\tau_0)$] has simple zeros in τ_0 and is independent of α, then for $\alpha > 0$ sufficiently small the perturbed system (2.27) exhibits chaos in the sense of Smale horseshoes.

This theorem will now be applied to M_+ and M_- separately.

A. The M_+ case

From (3.4) and (3.5),

$$v^0_+(\tau) = \sin\phi^0_+(\tau) = \operatorname{sech}\tau \tag{3.10}$$

and

$$\sin 2\phi^0_+(\tau) = -2\operatorname{sech}\tau\tanh\tau \tag{3.11}$$

and hence

$$\begin{aligned} M_+(\tau_0) &= \int_{-\infty}^{\infty} v^0_+(\tau)\{-v^0_+(\tau) + \cot\theta \sin\phi^0_+(\tau) + (\xi/2)\cos[\bar{\omega}(\tau+\tau_0)]\sin 2\phi^0_+(\tau)\} d\tau \\ &= \int_{-\infty}^{\infty} (\cot\theta - 1)\operatorname{sech}^2\tau \, d\tau - \xi \int_{-\infty}^{\infty} \cos[\bar{\omega}(\tau+\tau_0)]\operatorname{sech}^2\tau\tanh\tau \\ &= 2(\cot\theta - 1) - \xi I \ , \end{aligned} \tag{3.12}$$

where I is the second integral in the preceding line. Integrating by parts yields

$$\begin{aligned} I &= -\frac{\bar{\omega}}{2}\int_{-\infty}^{\infty} \sin[\bar{\omega}(\tau+\tau_0)]\operatorname{sech}^2\tau \, d\tau \\ &= -\frac{\bar{\omega}}{2}\cos(\bar{\omega}\tau_0)\int_{-\infty}^{\infty} \sin(\bar{\omega}\tau)\operatorname{sech}^2\tau \, d\tau \\ &\quad -\frac{\bar{\omega}}{2}\sin(\bar{\omega}\tau_0)\int_{-\infty}^{\infty} \cos(\bar{\omega}\tau)\operatorname{sech}^2\tau \, d\tau \ . \end{aligned} \tag{3.13}$$

The first integrand in (3.13) is odd in τ and therefore its integral is zero; the second integral may be evaluated to give ([15], p. 505)

$$I = -\pi\frac{\bar{\omega}^2}{2}\sin(\bar{\omega}\tau_0)\operatorname{csch}(\bar{\omega}\pi/2) \ . \tag{3.14}$$

The insertion of (3.14) into (3.12) finally shows

$$M_+(\tau_0) = \xi\pi\frac{\bar{\omega}^2}{2}\operatorname{csch}(\bar{\omega}\pi/2)[R_+(\bar{\omega},\theta)/\xi + \sin(\bar{\omega}\tau_0)] \ , \tag{3.15}$$

where

$$R_+(\bar{\omega},\theta) = [4/(\bar{\omega}^2\pi)](\cot\theta - 1)\sinh(\bar{\omega}\pi/2) \ . \tag{3.16}$$

It is clear from (3.15) that $M_+(\tau_0)$ has simple zeros in τ_0 provided

$$|R_+(\bar{\omega},\theta)| < \xi \ . \tag{3.17}$$

Hence, by the Melnikov theorem stated above, whenever condition (3.17) is satisfied it can be deduced that for sufficiently small α the system (2.27) [and hence Eq. (2.20)] exhibits chaos. As ξ increases in (3.17) (i.e., as the strength of the ac field increases) it is clear that larger ranges from the combined values of $\bar{\omega}$ and θ lead to chaotic solutions. Solving the equation $|R_+(\bar{\omega},\theta)| = \xi$ provides the boundary of the region in the $\bar{\omega}\theta$ plane inside which the corresponding values of $\bar{\omega}$ and θ force R_+ to fulfill (3.17), and hence produce chaos. Writing

$$R_+(\bar{\omega},\theta) = F(\bar{\omega})(\cot\theta - 1) \ , \tag{3.18}$$

where

$$F(\bar{\omega}) = 4\sinh(\bar{\omega}\pi/2)/(\bar{\omega}^2\pi) \ , \tag{3.19}$$

it is seen that $F(\bar{\omega})$ has a global minimum at

$$\bar{\omega}_c = (4/\pi)\tanh(\bar{\omega}_c\pi/2) = 1.219 \tag{3.20}$$

with

$$F(\bar{\omega}_c)=2.844\ . \tag{3.21}$$

As θ tends to $\pi/2$, $|R_+(\bar{\omega},\theta)|\to F(\bar{\omega})$ and therefore there is a critical value of ξ, namely,

$$\xi_c=F(\bar{\omega}_c)=2.844 \tag{3.22}$$

for which the chaotic regime is extended to also include $\theta=\pi/2$. For the lower branch of the curve enclosing the chaotic regime we can derive an approximate condition being valid close to the minimum of the curve provided θ is small. In this case $\cot\theta-1\approx\cot\theta\approx 1/\theta$. The condition (3.17) can now, using (3.18), be written as

$$\theta>F(\bar{\omega})/\xi\ , \tag{3.23}$$

where $F(\bar{\omega})$ is given by Eq. (3.19). Thus the smallest value of θ producing chaos for a given $\xi\gg 2.844$ will occur for $\bar{\omega}=\bar{\omega}_c$ and the corresponding value of θ is given by

$$\theta_c=F(\bar{\omega}_c)/\xi\approx 2.844/\xi\ . \tag{3.24}$$

In Fig. 4 are depicted the curves enclosing the corresponding values of $\bar{\omega}$ and θ leading to chaos for some different values of ξ. Two of the curves ($\xi=1,2.8$) represent $\xi<\xi_c$, and the largest possible value of θ leading to chaos is less than $\pi/2$. When increasing ξ the possible combinations of $\bar{\omega}$ and θ producing chaos expands. For the four curves ($\xi=3.2,8,28.44,100$) $\xi>\xi_c$ and we see how ultimately the whole $\bar{\omega}\theta$ plane will produce chaos in the limit as $\xi\to\infty$.

B. The M_- case

Replacing $\mathbf{q}_+^0$ by $\mathbf{q}_-^0$ in Eq. (3.8) leads to the same calculations as those carried out above for the M_+ case, the only difference being changes in the signs of certain integrals due to (3.4) and (3.6), for example,

$$v_-^0(\tau)=-\sin\phi_-^0(\tau)=-\operatorname{sech}\tau\ , \tag{3.25}$$

$$\sin 2\phi_-^0(\tau)=2\operatorname{sech}\tau\tanh\tau\ . \tag{3.26}$$

The resulting Melnikov function is

$$M_-(\tau_0)=-\xi\pi\frac{\bar{\omega}^2}{2}\operatorname{csch}(\bar{\omega}\pi/2)\times[R_-(\bar{\omega},\theta)/\xi-\sin(\bar{\omega}\tau_0)]\ , \tag{3.27}$$

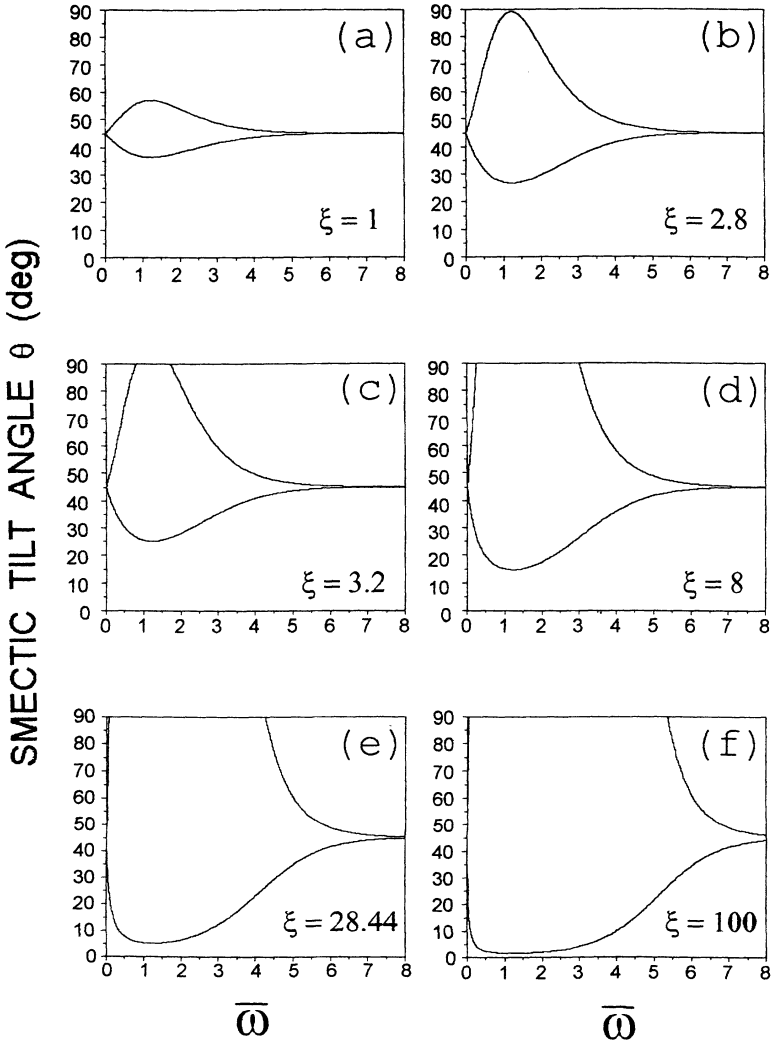

FIG. 4. Plots of $|R_+(\bar{\omega},\theta)|=\xi$ in the $\bar{\omega}\theta$ plane, $\bar{\omega}$ being the rescaled frequency of the ac field and θ the smectic tilt angle depicted in Fig. 1; ξ is related to the strength of the ac field by Eq. (2.18). Combinations of $\bar{\omega}$ and θ inside these boundaries lead to chaotic instabilities. The critical value of ξ for which θ can first (theoretically) be 90° for chaotic solutions is $\xi_c=2.844$, with frequency $\bar{\omega}_c=1.219$. As ξ increases, the boundary $|R_+|=\xi$ expands, allowing further combinations of $\bar{\omega}$ and θ which lead to chaos.

where

$$R_-(\bar{\omega},\theta)=[4/(\bar{\omega}^2\pi)](\cot\theta+1)\sinh(\bar{\omega}\pi/2)\ . \quad (3.28)$$

In a similar manner to the M_+ case above, $M_-(\tau_0)$ has simple zeros in τ_0 whenever

$$|R_-(\bar{\omega},\theta)|<\xi \quad (3.29)$$

and hence, by the Melnikov theorem, condition (3.29) is sufficient to ensure that for sufficiently small α the system (2.27) exhibits chaos. As in the previous case, solving $|R_-(\bar{\omega},\theta)|=\xi$ gives the boundary of the region in the $\bar{\omega}\theta$ plane inside which the corresponding values of $\bar{\omega}$ and θ lead to chaos, by Eq. (3.29). Setting

$$R_-(\bar{\omega},\theta)=F(\bar{\omega})(\cot\theta+1)\ , \quad (3.30)$$

where F is given by (3.19), we can see, since R_- is always positive, that for all θ

$$R_-(\bar{\omega},\theta)\geq F(\bar{\omega}_c)\ , \quad (3.31)$$

where $\bar{\omega}_c$ and $F(\bar{\omega}_c)$ are given in (3.20) and (3.21). Hence chaotic solutions are only possible in this case when $\xi>\xi_c=2.844$. The relevant combinations of chaos producing values for $\bar{\omega}$ and θ lie above the curve $R_-(\bar{\omega},\theta)=\xi$, as shown in Fig. 5. In this figure four different values of ξ ($\xi=3.2,8,28.44,100$) have been used in the calculations, showing the expansion in possible values for $\bar{\omega}$ and θ producing chaos as ξ increases above ξ_c.

C. Remarks

In both the M_+ and M_- cases increasing the controlling parameter ξ for the ac field will force the region in the $\bar{\omega}\theta$ plane for which chaos occurs to expand in area. This leads to the interpretation that chaos is more likely to be present in the given sample under a higher-strength ac electric field. The M_+ calculation involving the relation (3.17) is relevant when the initial perturbation corresponds to a small change in the initial data above the ϕ axis close to the $\mathbf{q}_+^0$ unperturbed orbit in the phase plane. Similarly, the M_- calculation and Eq. (3.29) are relevant for small changes to the initial data below the ϕ axis close to the unperturbed $\mathbf{q}_-^0$ orbit.

As discussed above, when $\xi<\xi_c\approx 2.844$ only the M_+ calculations produce chaotic solutions. When, on the other hand, $\xi>\xi_c$ both the M_+ and M_- calculations produce chaos. It can be deduced from Eqs. (3.17), (3.18), (3.29), and (3.30) that the region in the $\bar{\omega}\theta$ plane for which the M_- calculation produces chaos is always contained within the chaotic region of the M_+ calculation. (This result is clearly demonstrated by Figs. 4 and 5.) Thus, in order to establish the existence of chaotic solutions, performing the M_+ calculation is sufficient. However, if we are also interested in the type of perturbations which can be involved in the chaotic solutions, we would also have to carry out the M_- calculations.

IV. DISCUSSION

In this article we have shown that there exist chaotic solutions to the continuum equations for planar aligned nonchiral smectic-C liquid crystals whenever a static electric field augmented by a suitably weak ac field is applied at a small oblique angle to the smectic layers. The instability which arises in the movement of the c director is analogous to the motion of a pendulum near its unstable equilibrium: any small perturbation may cause the pendulum to fall in a complicated chaotic fashion. Similarly, small perturbations of certain positions of the c

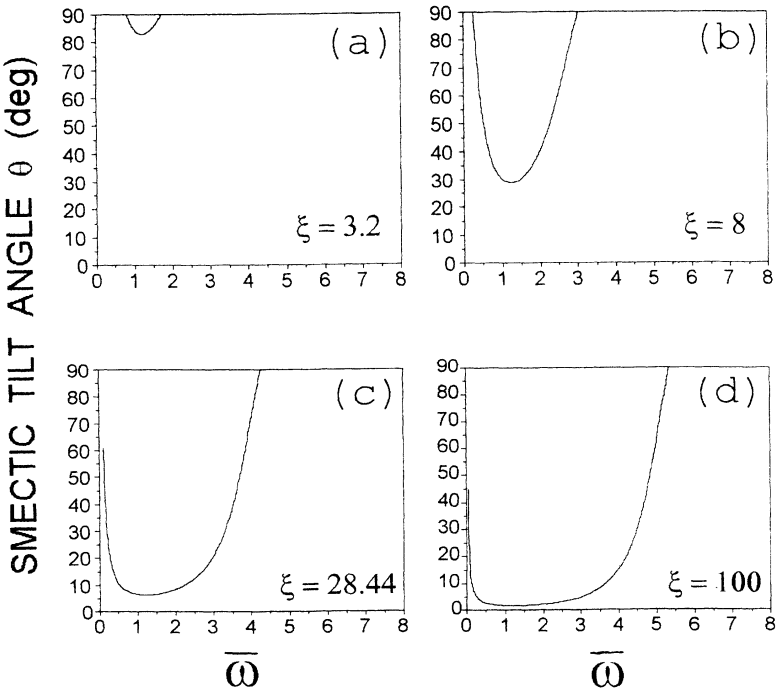

FIG. 5. Plots of $|R_-(\bar{\omega},\theta)|=\xi$ in the $\bar{\omega}\theta$ plane, $\bar{\omega}$ being the rescaled frequency of the ac field and θ the smectic tilt angle depicted in Fig. 1; ξ is related to the strength of the ac field by Eq. (2.18). Chaotic solutions are only available for $\xi>\xi_c=2.844$; these solutions first occur when ξ is close to ξ_c and $\bar{\omega}$ is close to $\bar{\omega}_c=1.219$. The area above the curves represent combinations of $\bar{\omega}$ and θ which lead to chaos. Increasing ξ allows more chaos-producing combinations of $\bar{\omega}$ and θ.

director lead to initially chaotic motion. The control parameters probing the instability in an experiment are the tilt angle θ, the angle α between the electric field and the smectic planes, and the strength E_0^{ac} and frequency f of the ac field. For mathematical reasons we have not introduced E_0^{ac} and f when performing the calculations but instead the quantities ξ and $\bar{\omega}$, which are defined by Eqs. (2.18) and (2.24). From Eq. (2.17) we notice that

$$E_0^{ac}=\tfrac{1}{2}\varepsilon E_0 \ , \tag{4.1}$$

$$2\pi f=\omega\varepsilon \ . \tag{4.2}$$

By Eq. (2.13) we introduced t_0, which represents a typical time scale for the problem. The corresponding frequency is given by $f_0=1/t_0$ and we now introduce a dimensionless frequency $\bar{f}$ by the relation

$$\bar{f}=f/f_0=ft_0 \ . \tag{4.3}$$

As control parameter when presenting the results we will now instead of ξ and $\bar{\omega}$ (which are used in Figs. 4 and 5) choose ε, which is twice the ratio between the amplitudes of the ac and static electric fields and the dimensionless frequency $\bar{f}$. By using Eqs. (2.18), (2.25), (4.2), and (4.3) one can express the more physically related control parameters ε and $\bar{f}$ in terms of ξ and $\bar{\omega}$ as

$$\varepsilon=\xi\alpha \ , \tag{4.4}$$

$$\bar{f}=\frac{\bar{\omega}\alpha\sin^2\theta}{2\pi} \ . \tag{4.5}$$

In order to investigate which parameter values will lead to chaotic behavior of the system we only have to investigate the M_+ case for the reasons explained in Sec. III C above. Figure 6 shows how the chaotic region in the $\bar{f}\theta$ plane expands with increasing ε for $\alpha=1°$ and 5°. As the calculated results, depicted in Fig. 4, are universal in ξ and $\bar{\omega}$, we see from Eqs. (4.4) and (4.5) that whenever ε/α is the same the chaotic region will be unchanged if we replace $\bar{f}$ by $\bar{f}/\alpha$. Thus when α decreases the chaotic region will be pushed down to smaller frequencies and ulti-

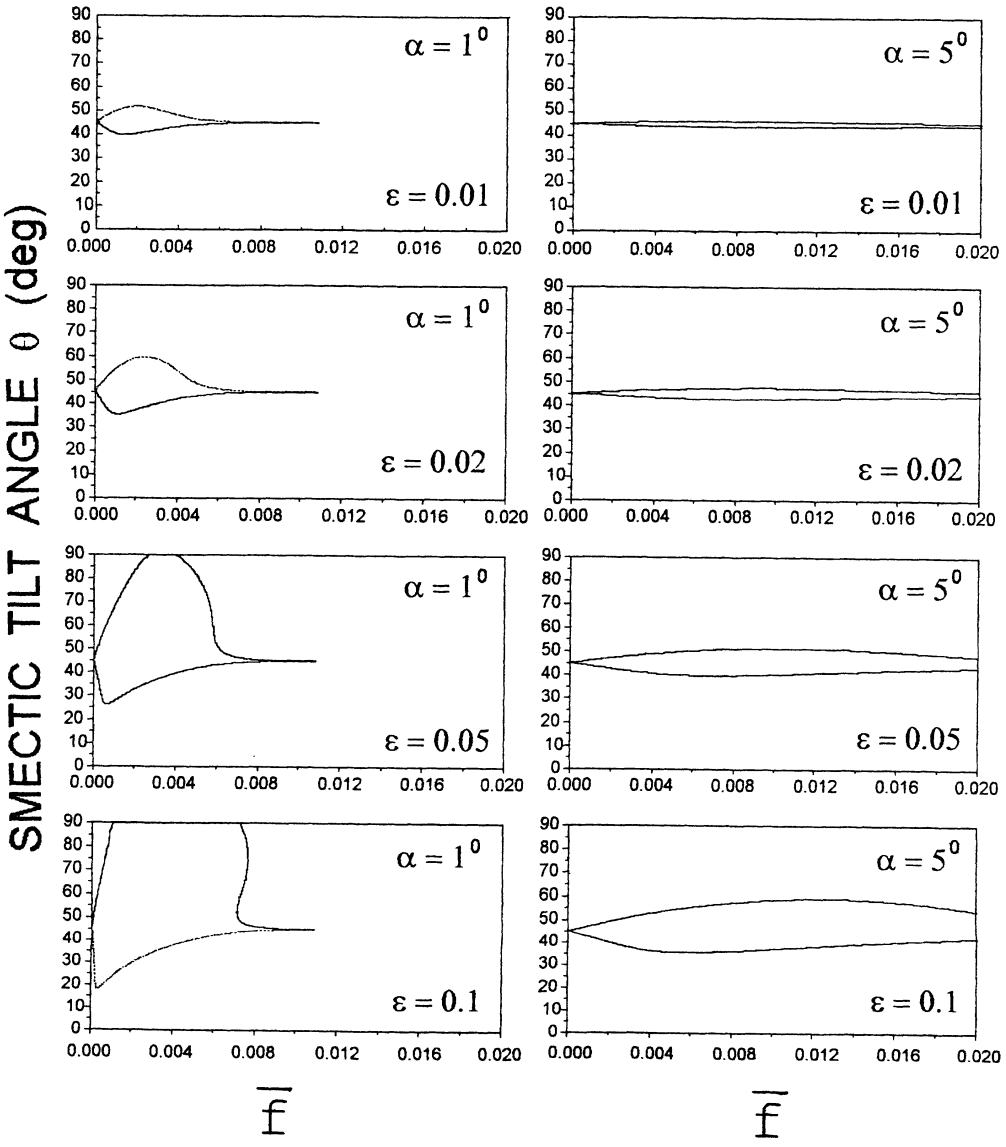

FIG. 6. Chaotic regime in the $\bar{f}\theta$ plane for various combinations of the angle α between the applied electric field and the layer normal and the reduced electric field ε, discussed in Sec. IV.

mately disappear in the limit as $\alpha \to 0$. The typical frequencies $\bar{f}$ for which chaos appears are seen in Fig. 6 to be $\bar{f} \approx 0.01$. If the typical response time of the system, t_0, is taken to be $t_0 \approx 1$ ms, we conclude that a typical frequency for which chaotic behavior can be expected to occur is $f = \bar{f}/t_0 \approx 100$ Hz. Generally, as the estimation made above is very rough, we would thus expect observations of chaos to be possible whenever the frequency of the applied field is in the low-Hz region ($10^{-2} < f < 10^5$ Hz).

In the geometrical setup described in Sec. II A, the ac field introduced has a small amplitude and slow frequency; as an alternative, E in Eq. (2.17) could be replaced by

$$E_0 \to E_0[1+(\varepsilon/2)\cos(\omega t)] , \tag{4.6}$$

but this rescales $\bar{\omega}$ to $\omega \xi t_0/(\alpha \sin^2\theta)$ and the resulting M_+ (or M_-) Melnikov function becomes α dependent, thereby invalidating the use of the Melnikov theorem. An attempt to overcome this kind of particular problem, as mentioned by Marsden [13], may be made by examining suitable expansions of the stable and unstable manifolds for the perturbed equations and carrying out a more detailed error analysis in the resulting ε expansions. It is conjectured that such an approach is possible and will yield further existence results for chaos.

The subharmonic orbits which are present in the phase plane (for example, the periodic orbits around $\phi = \pi/2$) may be calculated explicitly for the unperturbed system (3.1). An application of the subharmonic Melnikov function, which (unlike the Melnikov function introduced above) is based on these orbits, their periods and other relevant behavior, may establish whether or not any of them survive as perturbed periodic orbits (having different periods) when $\alpha > 0$ is small; the stability of such perturbed periodic orbits may also be examined (see Stewart and Carlsson [16]).

To summarize, in this paper we have shown how the motion of the domain walls described in Sec. II A with suitable arrangements can become chaotic. The main results of the paper are shown in Figs. 4–6. From Fig. 6 it is seen how, for a given value of the angle α between the oblique electric field and the smectic planes, the region in the $\bar{f}\theta$ plane for which chaotic motion appears will grow with increasing field strength ε of the ac electric field. In an experiment performed at a certain temperature, the tilt angle θ can be considered to be constant unless the system is very close ($T_c - T < 1$ K) to the smectic-A–smectic-C phase-transition temperature [17]. If, for given α and ε, the frequency $\bar{f}$ of the ac field is increased, the system will follow a horizontal line in the $\bar{f}\theta$ plane as depicted in Fig. 7. Provided $\theta > \theta_c$ there will be an interval $\bar{f}_1 < \bar{f} < \bar{f}_2$ in the frequency for which chaotic behavior of the system is expected. For these frequencies the nature of the motion of the domain walls is unpredictable and nonrepeatable.

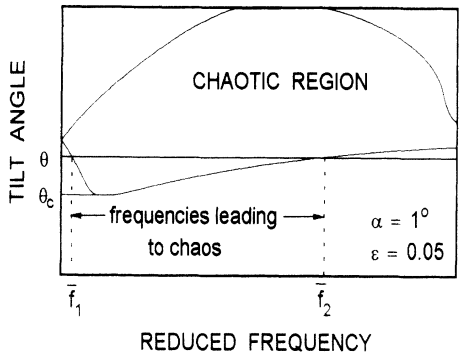

FIG. 7. Chaotic regime in the $\bar{f}\theta$ plane for $\alpha = 1°$ and $\varepsilon = 0.05$. If $\theta > \theta_c$ and the reduced frequency $\bar{f}$ of the ac electric field is increased gradually, one sees how there will be an interval $\bar{f}_1 < \bar{f} < \bar{f}_2$ for which the motion of the domain wall is chaotic.

Another system for which the investigation of chaotic behavior might be of interest is the switching of a surface-stabilized ferroelectric liquid-crystalline (SSFLC) cell. In these cells a chiral smectic-C liquid crystal is switching between two configurations, driven by an electric field. Superimposed on the switching field one normally applies a background high-frequency ac electric field. In reality, one must always expect the angle between the smectic planes and the applied electric field to be nonzero, either by the presence of chevrons or by imperfections of the alignment of the smectic layers. Thus there is the possibility that chaotic behavior can appear in the SSFLC cell if the values of the control parameters match in such a way that the system enters the chaotic region.

In conclusion, we hope that the techniques presented in this paper will allow a more detailed investigation of possible instabilities arising in other, more complicated smectic configurations across which an ac electric field is applied. We also hope that the work presented here might encourage some experimental efforts in studying the possible chaotic motion which can appear in the system studied in this paper.

APPENDIX

In this Appendix the theory introduced by Leslie and co-workers [3,4] is applied to the problem outlined in Sec. II, the reader being referred to these references for full information and details. From [3], the bulk energy integrand may be written in either of the two equivalent forms

$$\begin{aligned} 2w = {} & A_{12}(\mathbf{b}\cdot\nabla\times\mathbf{c})^2 + A_{21}(\mathbf{c}\cdot\nabla\times\mathbf{b})^2 + 2A_{11}(\mathbf{b}\cdot\nabla\times\mathbf{c})(\mathbf{c}\cdot\nabla\times\mathbf{b}) \\ & + B_1(\nabla\cdot\mathbf{b})^2 + B_2(\nabla\cdot\mathbf{c})^2 + B_3[\tfrac{1}{2}(\mathbf{b}\cdot\nabla\times\mathbf{b}+\mathbf{c}\cdot\nabla\times\mathbf{c})]^2 \\ & + 2B_{13}(\nabla\cdot\mathbf{b})[\tfrac{1}{2}(\mathbf{b}\cdot\nabla\times\mathbf{b}+\mathbf{c}\cdot\nabla\times\mathbf{c})] + 2C_1(\nabla\cdot\mathbf{c})(\mathbf{b}\cdot\nabla\times\mathbf{c}) + 2C_2(\nabla\cdot\mathbf{c})(\mathbf{c}\cdot\nabla\times\mathbf{b}) \qquad \text{(A1a)} \\ = {} & A_{21}(\nabla\cdot\mathbf{a})^2 + B_1(\mathbf{a}\cdot\nabla\times\mathbf{c})^2 + B_2(\nabla\cdot\mathbf{c})^2 + B_3(\mathbf{c}\cdot\nabla\times\mathbf{c})^2 \\ & + (2A_{11}+A_{12}+A_{21}+B_3)(\mathbf{b}\cdot\nabla\times\mathbf{c})^2 - (2A_{11}+2A_{21}+B_3)(\nabla\cdot\mathbf{a})(\mathbf{b}\cdot\nabla\times\mathbf{c}) \\ & - 2B_{13}(\mathbf{a}\cdot\nabla\times\mathbf{c})(\mathbf{c}\cdot\nabla\times\mathbf{c}) + 2(C_1+C_2-B_{13})(\nabla\cdot\mathbf{c})(\mathbf{b}\cdot\nabla\times\mathbf{c}) - 2C_2(\nabla\cdot\mathbf{a})(\nabla\cdot\mathbf{c}) , \qquad \text{(A1b)} \end{aligned}$$

where A_i, B_i, and C_i are elastic constants related to those given by the Orsay Liquid Crystal Group [18] (OLCG) (the only changes being $A_{11}=-\frac{1}{2}A_{11}^{\mathrm{OLCG}}$ and $C_1=-C_1^{\mathrm{OLCG}}$) and $\mathbf{b}=\mathbf{a}\times\mathbf{c}$, surface terms being omitted. From [4], the balance of angular momentum leads to the following Euler-Lagrange equations in Cartesian component form for **a** and **c**, respectively, where W is the sum of the bulk energy (A1b) and the electric energy at (2.7):

$$\left[\frac{\partial W}{\partial(a_{i,j})}\right]_{,j}-\frac{\partial W}{\partial a_i}+g_i^a+\lambda a_i+\mu c_i+e_{ijk}\beta_{k,j}=0\ , \tag{A2}$$

$$\left[\frac{\partial W}{\partial(c_{i,j})}\right]_{,j}-\frac{\partial W}{\partial c_i}+g_i^c+\chi c_i+\mu a_i=0 \tag{A3}$$

for $i=1,2,3$, where, for example, $a_{i,j}$ denotes partial differentiation of the ith component of **a** with respect to the jth variable. The usual alternator is represented by e_{ijk}, while repeated indices follow the summation convention and are summed from 1 to 3. The four constraints (2.1) and (2.2) lead to the introduction of the Lagrange multipliers λ, μ, χ, and $\boldsymbol{\beta}$ which appear in Eqs. (A2) and (A3), the multiplier μ linking the two sets of equations for the a and c directors. The terms $\mathbf{g}^a$ and $\mathbf{g}^c$ are the dynamic contributions related to **a** and **c**, respectively, arising from the dynamic stress tensor formulated in [4]. From Eqs. (3.19) and (3.20) in [4], the dynamic contributions $\mathbf{g}^a$ and $\mathbf{g}^c$ appearing in the above equations are

$$g_i^a=-2\tau_5\frac{\partial c_i}{\partial t}\ , \tag{A4}$$

$$g_i^c=-2\lambda_5\frac{\partial c_i}{\partial t}\ , \tag{A5}$$

where τ_5 and λ_5 are viscosity coefficients, λ_5 being the positive (see [4]) rotational viscosity related to the movement of the director **n** around a cone. Upon inserting (A4) and (A5) into (A2) and (A3) an evaluation or elimination of the Lagrange multipliers can be pursued, thereby arriving at the equation that governs the movement of the c director.

Since the equations examined in Sec. II are only z and t dependent, the substitution of the energy W given by adding (A1b) and (2.7) into (A2) and (A3) yields for our given ansatz, respectively,

$$\varepsilon_a\varepsilon_0E_0(\sin\alpha\cos\theta+\cos\alpha\sin\theta\cos\phi)\cos\theta E_i-2\tau_5\frac{\partial c_i}{\partial t}+B_{13}c_i\left[\frac{\partial\phi}{\partial z}\right]^2+\lambda a_i+\mu c_i+e_{ijk}\beta_{k,j}=0\ , \tag{A6}$$

$$B_3c_{i,33}-B_3c_i\left[\frac{\partial\phi}{\partial z}\right]^2+\varepsilon_a\varepsilon_0E_0(\sin\alpha\cos\theta+\cos\alpha\sin\theta\cos\phi)\sin\theta E_i-2\lambda_5\frac{\partial c_i}{\partial t}+\chi c_i+\mu a_i=0 \tag{A7}$$

for $i=1,2,3$. On account of (2.1) and (2.5),

$$a_i\frac{\partial c_i}{\partial t}=0 \tag{A8}$$

and therefore taking the scalar product of (A7) with **a** shows

$$\mu=-\varepsilon_a\varepsilon_0E_0^2(\sin\alpha\cos\theta+\cos\alpha\sin\theta\cos\phi)\sin\theta\sin\alpha\ . \tag{A9}$$

We now seek the multipliers λ and $\boldsymbol{\beta}$. It is known that for any $\mathbf{A}\in C^2(\mathbb{R}^3)$

$$\operatorname{div}\mathbf{A}=0 \quad\text{if and only if}\quad \mathbf{A}=\nabla\times\mathbf{B} \tag{A10}$$

for some $\mathbf{B}\in C^2(\mathbb{R}^3)$ (unique, apart from a constant) and therefore equation (A6) may be solved for suitable λ and $\boldsymbol{\beta}$ by taking the divergence of (A6) and solving for a possible λ; such a λ will ensure the existence of a vector multiplier $\boldsymbol{\beta}$ through the relation (A10) which, for our present purposes, need not be derived explicitly. Substituting μ from (A9) into (A6) and taking the divergence gives

$$\lambda_{,3}=\mu_{,3}\cot\theta \tag{A11}$$

from which we may clearly set

$$\lambda=\mu\cot\theta\ , \tag{A12}$$

the existence of $\boldsymbol{\beta}$ being guaranteed by (A10). It now follows that solving for **c** in (A7) (that is, solving for ϕ) also allows us to completely solve the equations for **a** given by (A6).

The multiplier χ will now be eliminated from Eqs. (A7). Clearly, (A7) is satisfied for $i=3$ with the above choice of μ. For $i=2$,

$$B_3 c_{2,33} - B_3 c_2 \left[\frac{\partial \phi}{\partial z} \right]^2 - 2\lambda_5 \frac{\partial c_2}{\partial t} + \chi c_2 = 0 \tag{A13}$$

and for $i=1$,

$$B_3 c_{1,33} - B_3 c_1 \left[\frac{\partial \phi}{\partial z} \right]^2 + \varepsilon_a \varepsilon_0 E_0^2 (\sin\alpha \cos\theta + \cos\alpha \sin\theta \cos\phi) \cos\alpha \sin\theta - 2\lambda_5 \frac{\partial c_1}{\partial t} + \chi c_1 = 0 \ . \tag{A14}$$

By multiplying (A13) by c_1 and (A14) by c_2, the multiplier χ can be eliminated by subtracting the equations to find

$$B_3 \frac{\partial^2 \phi}{\partial z^2} - 2\lambda_5 \frac{\partial \phi}{\partial t} = \varepsilon_a \varepsilon_0 E_0^2 (\sin\alpha \cos\theta + \cos\alpha \sin\theta \cos\phi) \cos\alpha \sin\theta \sin\phi \ . \tag{A15}$$

[1] P. G. de Gennes, *The Physics of Liquid Crystals* (Clarendon, Oxford, 1974).

[2] T. Carlsson, I. W. Stewart, and F. M. Leslie, Liq. Cryst. **9**, 661 (1991).

[3] F. M. Leslie, I. W. Stewart, T. Carlsson, and M. Nakagawa, Continuum Mech. Thermodyn. **3**, 237 (1991).

[4] F. M. Leslie, I. W. Stewart, and M. Nakagawa, Mol. Cryst. Liq. Cryst. **198**, 443 (1991).

[5] I. W. Stewart and N. Raj, Mol. Cryst. Liq. Cryst. **185**, 47 (1990).

[6] P. Schiller, G. Pelzl, and D. Demus, Liq. Cryst. **2**, 21 (1987).

[7] M. Nakagawa, J. Phys. Soc. Jpn. **59**, 81 (1990).

[8] I. W. Stewart, M. Nakagawa, and F. M. Leslie (unpublished).

[9] F. Kh. Abdullaev, A. A. Abdumalikov, and E. N. Tsoi, Phys. Status Solidi B **146**, 457 (1988).

[10] C. W. Oseen, Trans. Faraday Soc. **29**, 883 (1933).

[11] T. Carlsson, F. M. Leslie, and N. A. Clark (unpublished).

[12] J. Guckenheimer and P. Holmes, *Nonlinear Oscillations, Dynamical Systems, and Bifurcation of Vector Fields* (Springer-Verlag, New York, 1983).

[13] J. E. Marsden, in *Chaos in Nonlinear Dynamical Systems*, edited by J. Chandra (SIAM, Philadelphia, 1984).

[14] S. Wiggins, *Chaotic Transport in Dynamical Systems* (Springer-Verlag, New York, 1992).

[15] I. S. Gradshteyn and I. W. Ryzhik, *Tables of Integrals, Series and Products* (Academic, New York, 1965).

[16] I. W. Stewart and T. Carlsson (unpublished).

[17] T. Carlsson and I. Dahl, Mol. Cryst. Liq. Cryst. **95**, 373 (1983).

[18] Orsay Liquid Crystal Group, Solid State Commun. **9**, 653 (1971).